

## Ionization and recombination rates for argon ions Ar XII–XVI from time-resolved spectroscopy of tokamak plasmas

Jieh-Shan Wang and Hans R. Griem

*Laboratory for Plasma and Fusion Energy Studies, University of Maryland, College Park, Maryland 20742*

William L. Rowan

*Fusion Research Center, The University of Texas, Austin, Texas 78712*

(Received 16 March 1987)

The effective ionization and recombination rate coefficients Ar XII–XVI were obtained by studying the modulation of line emission by sawtooth oscillations in the Texas Experimental tokamak (TEXT). Experimental data are matched with the simulation of argon ion emission by a one-dimensional code. The rate coefficients were determined for  $T_e \sim 400$  eV and  $N_e \sim 4 \times 10^{13}$  cm $^{-3}$ . The uncertainty of ionization rates is estimated to be less than 30%, while the accuracy of the recombination rates is better than a factor of 2.

### I. INTRODUCTION

Ionization and recombination rate coefficients are important atomic data for calculations of the ionic balance in plasmas. In fusion plasmas the rates are required for studies of impurity transport and power balance. In laser-produced plasmas and dense z-pinch plasmas the rates are required for calculation of ionic abundances that are important for interpretation of observed radiation from these plasmas. Corresponding cross sections are often obtained from approximate theories, with experimental checks from crossed beam experiments being still rare and sometimes less direct than anticipated. Most direct measurements of atomic rate coefficients have been done in theta-pinch devices.<sup>1,2</sup> Because of the limitation in electron temperature in theta pinches, they can only be used to study ions of relatively low charge state. For highly ionized ions, measurements of effective rate coefficients can be done in tokamaks at higher electron temperature, the ions being an intrinsic impurity or introduced artificially.<sup>3</sup>

Ionization and recombination rates for Mo XXXI were measured by Breton *et al.*<sup>4</sup> from observed sawtooth modulation of Mo XXXI and XXXII line emissions. Isler *et al.*<sup>5</sup> measured ratios of ionization and recombination rates for Fe XV–XIX in the ISX-B tokamak during counter injection of neutral beams. Recently, ionization and recombination rates for titanium ions Ti XVII–XX were measured in the Texas Experimental tokamak (TEXT) by Wang *et al.*<sup>6</sup> They extended the method of Breton *et al.* to include the effects of tokamak transport and temperature profile variations during the sawtooth cycle. A one-dimensional (1D) code was developed to simulate line emissions from the plasma for comparison with the experiment.

In this article we report the determination of ionization and recombination rate coefficients for highly ionized argon ions using the same method as described by Wang *et al.* The principle of the measurement will be discussed

only briefly in Sec. II, as a more detailed discussion of the principle and numerical method can be found in Ref. 6. Section III contains the experimental parameters and a brief description of the experiment. Section IV contains results and discussions of our measurement.

### II. PRINCIPLE OF THE MEASUREMENT

The  $m = 1$  tearing mode in a tokamak plasma causes changes in the electron temperature profile,<sup>7</sup> which can be readily observed from the sawtooth modulation of soft-x-ray signals. The change of the  $T_e$  profile can also vary the abundances of impurity ions. This can be observed in the modulation of line emission signals. While the temperature profile can flatten or even be hollow for a short time, as seen from the rapid crash in the soft-x-ray signals, the ionic abundances vary rather smoothly according to the processes of ionization and recombination. Thus there are time lags or phase differences in the soft-x-ray and line emission signals. The phases are affected by the ionization and recombination rates, and one can obtain the atomic rates from the observed phase differences. The phase differences can be seen from the correlations

$$C(\tau) = \frac{\int_0^T S(t)L(t+\tau)dt}{\left[ \int_0^T S(t)S(t)dt \right]^{1/2} \left[ \int_0^T L(t)L(t)dt \right]^{1/2}},$$

where  $S(t)$  is the soft-x-ray signal and  $L(t)$  is the line emission signal. A 1D code that solves the transport-ionization-recombination equation,

$$\frac{\partial N_k}{\partial t} = -\frac{1}{r} \frac{\partial(r\Gamma_k)}{\partial r} + N_e(S_{k-1}N_{k-1} - S_k N_k + \alpha_{k+1}N_{k+1} - \alpha_k N_k),$$

is used to calculate the ionic abundances. In the equation, the  $\Gamma_k$ 's are the particle fluxes, the  $S_k$ 's are the ionization rate coefficients, and the  $\alpha_k$ 's are the recombination-rate coefficients. The particle fluxes are

written as

$$\Gamma_k = - \left[ D(r) \frac{\partial N_k}{\partial r} + V(r) N_k \right],$$

where  $D(r)$  is the diffusion coefficient and  $V(r)$  is the convective velocity, both assumed to be independent of the ion species. Inputs for the code are the transport coefficients and the ionization and recombination rate coefficients. The diffusion coefficient is assumed to be constant at  $10^4 \text{ cm}^2 \text{ s}^{-1}$ . The convective velocity is assumed to be of the form  $V(r) = V(a)(r/a)$ , with  $V(a) = 10^3 \text{ cm/sec}$ , and  $a = 27 \text{ cm}$  is the minor radius. A sawtooth function inferred from the experiment is used to generate variations of the temperature profile which in turn causes variations in the rate coefficients. The assumed temperature profile is consistent with Thomson scattering and soft-x-ray diode-array measurements. The transport coefficients are values measured using the impurity-injection method.<sup>8</sup>

The ionization rate coefficients are calculated using Lotz's formula.<sup>9</sup> The recombination rate coefficients are the sum of the dielectronic rates from Burgess's formula,<sup>10</sup> with a correction for  $\Delta n > 0$  transitions,<sup>11</sup> and the radiative rates from a hydrogenic formula.<sup>12</sup> The rate coefficients are multiplied by adjustable multipliers. For Ar VIII–XI we also used the rate coefficients measured by Meng *et al.*<sup>13</sup> Since these ions are of little importance in our analysis, the results reported here remain the same.

The code calculates line emissions from ionic abundances and the correlations with the sawtooth oscillations are then calculated. These simulated correlations are compared with the experimental correlations. The rate coefficients are varied to achieve a better match of the two correlations. The rates are determined from the best match. Errors can be estimated from the sensitivity of the method to the variation of the input parameters.

### III. THE EXPERIMENT

The measurements of the argon-ion rate coefficients were done on the TEXT tokamak. One plasma condition was studied in this experiment, with plasma current of 300 kA and a toroidal magnetic field of 26 kG. Diagnostics include ECE (electron cyclotron harmonic emission), the TEXT silicon surface-barrier array, microwave interferometry, and vuv spectroscopy. The argon atoms were introduced by gas puffing. The line-averaged electron density was measured by microwave interferometry to  $\sim 5 \times 10^{13} \text{ cm}^{-3}$ . The sawtooth oscillation has an average period of  $\sim 4.2 \text{ ms}$ . The averaged electron temperature profile is of the form  $T_e(r) = T_e(0) \exp[-(r/b)^c]$ , where  $T_e(0) = 900 \text{ eV}$ ,  $b = 16.1 \text{ cm}$ , and  $c = 2.5$ . The electron density profile is of the form  $N_e(r) = N_e(0) \{0.9[1 - (r/a)^2] + 0.1\}$ .

The observed argon-ion spectral lines are listed in Table I. The spectrometers employed were a 2.2-m grazing-incidence monochromator and a 1-m normal-incidence monochromator. The spectrometers view the plasma along the central chord. The signals were digitized at 25 kHz sampling rate.

The correlations of line emission signals with the soft-

TABLE I. Observed spectral lines.

Ion	Lines ( $\text{\AA}$ )	Transitions
Ar XII	193.7	$2s^2 2p^3(^2D_{5/2}) - 2s 2p^4(^2D_{5/2})$
Ar XIII	249.1	$2s^2 2p^2(^3P_2) - 2s 2p^3(^3D_{2,3})$
Ar XIV	257.5	$2s^2 2p(^2P_{3/2}) - 2s 2p^2(^2D_{3/2,5/2})$
Ar XV	424.0	$2s^2(^1S_0) - 2s 2p(^3P_1)$
Ar XVI	353.9	$2s(^2S_{1/2}) - 2p(^2P_{3/2})$

x-ray signal are shown as solid curves in Fig. 1(a), the quantity  $\theta$  in this figure is the averaged phase shift. Because of high noise levels the normalized correlations have amplitudes of about 0.2 to 0.5. The background, however, has correlation amplitudes of less than 0.1.

### IV. RESULTS AND DISCUSSION

The matched correlations from the simulation are shown in Fig. 1(b). Effective ionization and recombination rate coefficients giving this match are listed in Tables

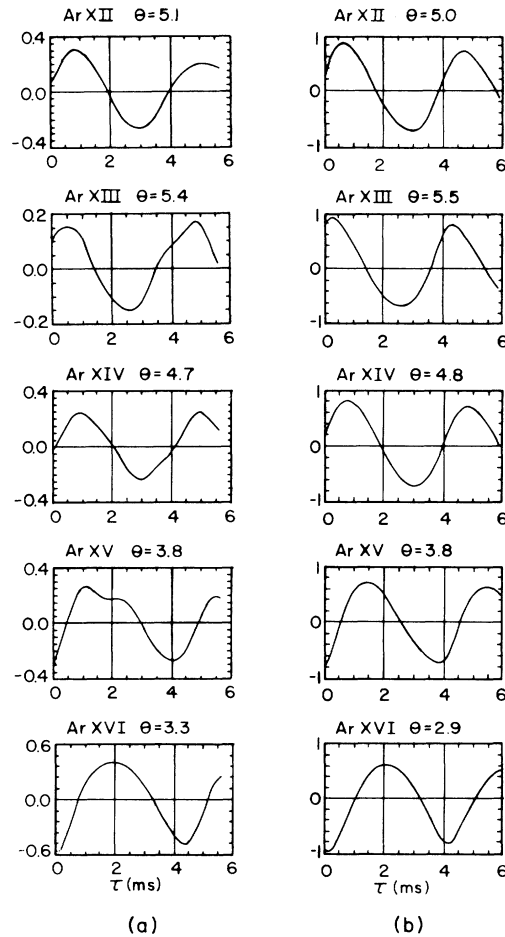


FIG. 1. (a) Experimental correlations for Ar XII–XVI. (b) Best matched theoretical correlations. The  $\theta$ 's are the phase shifts.

TABLE II. Effective ionization rate coefficients ( $10^{-11} \text{ cm}^3 \text{ s}^{-1}$ ).

Ion	$kT_e$ (eV)	$N_e$ ( $10^{13} \text{ cm}^{-3}$ )	$S_{\text{expt}}$	Lotz	GS
Ar XII	240	3.2	3.1	2.8	3.1
Ar XIII	340	3.7	3.7	3.7	4.6
Ar XIV	340	3.7	1.3	1.8	2.2
Ar XV	450	4.2	1.7	1.7	2.1
Ar XVI	560	4.5	1.2	1.0	1.2

II and III, respectively. The electron temperatures listed in the tables correspond to the values at the radius where each ion has its peak abundance. However, the ratios between experimental and theoretical rate coefficients are applicable at all radii. Rates from theoretical calculations are also listed in Tables II and III for comparison with our measurement.

Errors of the rate coefficients can be estimated by checking the sensitivity of the simulated correlations to the assumed values. It is found that a  $\pm 40\%$  simultaneous variation of all the ionization rates can cause phase changes of about 0.5 rad, which is larger than the errors in the experimental phases. The correlations are less sensitive to the changes in recombination rates. To cause significant changes in the phases of correlations one has to vary all rates by about 80%. Such estimation gives the possible range of the ionization and recombination rates.

One can also change the individual rates, which will cause correlations of the adjacent ion to change. We found that a change of a factor of 2 for the recombination rates can cause discernible variation in the correlations. For ionization rates the limit of detectable variation is 30%.

The values of ionization rate coefficients, except for Ar XIV, are close to the Lotz rates. The ionization rate coefficients (GS) calculated from the formula of Golden and Sampson<sup>14</sup> in general are higher than Lotz values. The experimental values of Ar XIV are about 40% less than the rates of Golden and Sampson.

The effective recombination rate coefficients  $\alpha'_{\text{eff}}$ , except

for Ar XIII, are also close to our theoretical recombination rate coefficients which are the sum of  $\alpha'_{\text{theor}}$  and  $\alpha'$  in Table III. The  $\alpha'_{\text{theor}}$  are our theoretical dielectronic recombination rate coefficients from Burgess's formula and the  $\alpha'$  are the radiative recombination rate coefficients which are less than 10% of  $\alpha'_{\text{theor}}$ , except for Ar XVI. The radiative rate coefficient for Ar XVI is about 30% of the dielectronic rate coefficient. On the contrary, the dielectronic rate coefficients  $\alpha'_{\text{SS}}$  by Shull and Van Steenberg<sup>15</sup> are lower for Ar XII, XV, and XVI, but in agreement for Ar XIII and XIV.

We like to point out that the dielectronic recombination rate coefficient for Ar XII, when extrapolated to 150 eV according to Burgess's formula, is in good agreement with the measurement of Meng *et al.*<sup>13</sup> The dielectronic rate coefficient for Ar XII measured by Meng *et al.* is  $2.4 \times 10^{-11} \text{ cm}^3 \text{ s}^{-1}$  and our result is  $2.7 \times 10^{-11} \text{ cm}^3 \text{ s}^{-1}$ . For Ar XV our measurement is also in good agreement with recent calculations by McLaughlin, LaGattuta, and Hahn.<sup>16</sup> The dielectronic rate coefficient they calculated is  $1.72 \times 10^{-11} \text{ cm}^3 \text{ s}^{-1}$  at about 450 eV. The measured dielectronic rate coefficient for Ar XVI is, however, smaller than the calculation of Roszman<sup>17</sup> by about 30%. Although there are differences between our measurement and various calculations, they are all within the measurement errors.

As was found in Ref. 6, the transport coefficients are not critical in our analysis. Detectable changes in the correlations require a variation of more than a factor of 2 of the used values.

TABLE III. Effective recombination rate coefficients.  $\alpha'_{\text{eff}}$  is the effective recombination rate coefficient determined from our experiment. The measured dielectronic recombination rate coefficient  $\alpha'_{\text{expt}}$  is  $\alpha'_{\text{eff}} - \alpha'$ .  $\alpha'$  is the calculated radiative recombination rate coefficient.  $\alpha'_{\text{theor}}$  is our calculation of the dielectronic rate coefficient using Burgess's formula. The rate coefficients are in units of  $10^{-11} \text{ cm}^3 \text{ s}^{-1}$ .

Ion	$kT_e$ (eV)	$N_e$ ( $10^{13} \text{ cm}^{-3}$ )	$\alpha'_{\text{eff}}$	$\alpha'$	$\alpha'_{\text{expt}}$	$\alpha'_{\text{theor}}$	$\alpha'_{\text{SS}}$
Ar XII	240	3.2	2.4	0.1	2.3	2.8	1.3
Ar XIII	340	3.7	1.4	0.1	1.3	2.3	1.4
Ar XIV	340	3.7	2.1	0.13	2.0	2.6	1.9
Ar XV	450	4.2	1.6	0.14	1.5	1.9	1.1
Ar XVI	560	4.5	0.67	0.14	0.53	0.42	0.24

## ACKNOWLEDGMENTS

We wish to thank A. J. Wootton, TEXT director, for his cooperation during this experiment; K. W. Gentle, R.

V. Bravenec, Burton Richard, and Kjell Nelin for operating TEXT; and the members of the TEXT Technical Staff for assisting in the setup. This work was supported by the U.S. Department of Energy.

- 
- <sup>1</sup>H. R. Griem, *J. Quant. Spectrosc. Radiat. Transfer* (to be published).
- <sup>2</sup>H.-J. Kunze, *Space Sci. Rev.* **13**, 565 (1972).
- <sup>3</sup>E. S. Marmor, J. L. Cecchi, and S. A. Cohen, *Rev. Sci. Instrum.* **46**, 1149 (1975).
- <sup>4</sup>C. Breton, C. DeMichelis, M. Finkenthal, and M. Mattioli, *Phys. Rev. Lett.* **41**, 110 (1978).
- <sup>5</sup>R. C. Isler, E. C. Crume, and D. E. Arnurius, *Phys. Rev. A* **26**, 2105 (1982).
- <sup>6</sup>J. S. Wang, H. R. Griem, R. Hess, W. L. Rowan, and T. P. Kochanski, *Phys. Rev. A* **33**, 4293 (1986).
- <sup>7</sup>R. E. Denton, J. F. Drake, R. G. Kleva, and D. A. Boyd, *Phys. Rev. Lett.* **56**, 2473 (1986).
- <sup>8</sup>W. L. Rowan *et al.*, *Bull. Am. Phys. Soc.* **28**, 1033 (1983).
- <sup>9</sup>W. Lotz, Institut für Plasmaphysik, Garching bei München, Report No. IPP 1/62, 1978 (unpublished).
- <sup>10</sup>A. Burgess, *Astrophys. J.* **141**, 1588 (1965).
- <sup>11</sup>A. L. Merts, R. D. Cowan, and N. H. Magee, Jr., Los Alamos Scientific Laboratory Report No. LA-6200-MS, 1976 (unpublished).
- <sup>12</sup>H. R. Griem, *Plasma Spectroscopy* (McGraw-Hill, New York, 1964), p. 160.
- <sup>13</sup>H. C. Meng, P. Greve, H.-J. Kunze, and T. Schmidt, *Phys. Rev. A* **31**, 3276 (1985).
- <sup>14</sup>L. B. Golden and D. H. Sampson, *J. Phys. B* **10**, 2229 (1977).
- <sup>15</sup>J. M. Shull and M. Van Steenberg, *Astrophys. J. Suppl.* **48**, 95 (1982).
- <sup>16</sup>D. J. McLaughlin, K. J. LaGattuta, and Y. Hahn, *J. Quant. Spectrosc. Radiat. Transfer* **37**, 47 (1987).
- <sup>17</sup>L. J. Roszman, *Phys. Rev. A* **35**, 2122 (1987).